

## Corrosion resistance of ultra fine-grained Ti

A. Balyanov<sup>a</sup>, J. Kutnyakova<sup>a</sup>, N.A. Amirkhanova<sup>a</sup>, V.V. Stolyarov<sup>a</sup>, R.Z. Valiev<sup>a</sup>,  
X.Z. Liao<sup>b</sup>, Y.H. Zhao<sup>b</sup>, Y.B. Jiang<sup>c</sup>, H.F. Xu<sup>c</sup>, T.C. Lowe<sup>b</sup>, Y.T. Zhu<sup>b,\*</sup>

<sup>a</sup> Institute of Physics of Advanced Materials, Ufa State Aviation Technical University, Ufa 450000, K. Marksa 12, Russia

<sup>b</sup> Materials Science and Technology Division, MS G755, Los Alamos National Laboratory, Los Alamos, NM 87545, USA

<sup>c</sup> Department of Earth and Planetary Science, University of New Mexico, NM 87131, USA

Received 26 August 2003; received in revised form 1 April 2004; accepted 10 April 2004

Available online 6 May 2004

### Abstract

We investigated the corrosion behavior of commercially pure (CP) Ti with both ultrafine-grained (UFG) and coarse-grained (CG) microstructures. It was found that the UFG Ti is more resistant to corrosion than its CG counterpart. The superior corrosion resistance of UFG Ti is believed to result from rapid passivation of UFG Ti and the impurity segregation to grain boundaries in CG Ti.

© 2004 Acta Materialia Inc. Published by Elsevier Ltd. All rights reserved.

**Keywords:** Equal channel angular pressing (ECAP); Titanium; Corrosion; Ultrafine grained microstructure

### 1. Introduction

In recent years, a variety of techniques for fabrication of ultrafine-grained (UFG) materials with grain sizes in the range of 10–1000 nm have been developed [1]. Most investigations on UFG materials have focused on thermal stability, microhardness, mechanical properties, and elastic properties [1]. The corrosion behavior of UFG materials has received only limited attention. Vinogradov et al. [2] have shown that the corrosion behavior of UFG Cu does not change significantly in comparison with coarse-grained (CG) polycrystalline Cu. Similarly, Rofagha et al. [3] have shown that the corrosion resistance is the same for CG and nanocrystalline nickel samples. In contrast, Rofagha et al. [4] also reported that the corrosion resistance of a nanocrystalline Ni–P alloy is lower than that for its CG counterpart. Thorpe et al. have revealed [5] that UFG materials may possess enhanced corrosion properties in comparison with their CG polycrystalline counterparts. For example, the nanocrystalline FeCr alloy has a considerably smaller corrosion current density in the active–passive region [6]. These reported results demonstrate that the effect of

nanostructuring on corrosion resistance varies among alloy systems.

The corrosion behavior of UFG Ti has not been investigated. It is the objective of this work to investigate the corrosion behavior of UFG Ti in comparison with its CG counterpart.

### 2. Material and experimental procedure

The composition of the UFG and CG Ti samples used in this study is (wt%) >99.36% Ti, <0.07% C, 0.18% Fe, 0.10% Si, 0.12% O, 0.04% N, 0.01% H and 0.3% other elements. The UFG Ti samples were processed by the equal channel angular pressing (ECAP) route Bc for 8 passes. Both the work piece and the ECAP die were preheated to 450 °C before the 1st pass and the temperature dropped to 400 °C after the 8th pass [7]. The as-processed Ti samples had an average grain size of 300 nm. The CG Ti samples were annealed at 800 °C in vacuum for 5 h, which resulted in an average grain size of 7 μm. To check the segregation of impurities to grain boundaries, we measured impurity contents on grain boundaries and interiors with X-ray energy dispersive spectroscopy (EDS) using a JEOL 2010F transmission electron microscope (TEM) equipped with an Oxford EDS system.

\* Corresponding author. Tel.: +1-505-667-4029; fax: +1-505-667-2264.

E-mail address: [yzhu@lanl.gov](mailto:yzhu@lanl.gov) (Y.T. Zhu).

We measured the corrosion potentials and the polarization curves in aerated 1M, 3M and 5M H<sub>2</sub>SO<sub>4</sub> solutions as well as 1M, 3M and 5M HCl solutions. All polarization curves were measured at a scan rate of 10<sup>-4</sup> V/s. The electrochemical cell was equipped with a reference electrode Ag–AgCl/saturated KCl, Pt counter electrode and Luggin capillary. Corrosion currents were determined from the polarization curves using a four-point method [8]. In addition, the corrosion rates were measured by a weight-loss method.

For the electrochemical measurements, the UFG and CG Ti samples were molded in Teflon, with a 3 mm in diameter window exposed to the solution. Just before an electrochemical measurement, the sample was mechanically polished and then electropolished in a freshly prepared solution consisting of 3 ml HNO<sub>3</sub> + 3 ml HF + 94 ml H<sub>2</sub>O, at a current density of 0.1 A/cm<sup>2</sup> and a voltage of 7 V for 3 min. The purpose of this pretreatment was to decrease surface defects. Samples were then rinsed with hot distilled water and alcohol. Upon immersion in the test solution, the sample was left for 30 min to achieve a steady open-circuit potential, which was measured as the corrosion potential.

The corrosion resistance was measured in a corrosion cell with acid solution re-circulation. The samples have a dimension of 25 mm in diameter and 10 mm in thickness. They were weighed before and after immersion in the corrosion cell at 35 °C for 2160 h (90 days). All the weight measurements were carried out with an analytical balance with an accuracy of 10<sup>-4</sup> g. The corrosion rate was calculated from the weight loss caused by corrosion.

### 3. Experimental results

#### 3.1. Corrosion potentials

The corrosion potentials of UFG and CG Ti in varying HCl and H<sub>2</sub>SO<sub>4</sub> acid solutions are listed in Table 1. Two trends can be seen from the data in Table 1: (1) the corrosion potentials for both UFG and CG Ti become more negative with increasing concentration of HCl or H<sub>2</sub>SO<sub>4</sub> acid; (2) the corrosion potentials of the UFG Ti are a little more positive than those for CG Ti in all cases. The differences are in the range of 1.1–8.8% and decreases with increasing concentration of hydrochloric or sulfuric acid.

#### 3.2. Polarization curves

Fig. 1 shows potentiostatic polarization curves of CG and UFG Ti obtained in HCl acid solutions. The definitions of passive current density,  $i_{\text{pass}}$ , primary passive potential  $E_P$ , and the critical current density,  $i_c$ , at  $E_P$  is shown Fig. 1a [9]. Several interesting features can be deduced from the curves, (i) the critical current density,  $i_c$ , for UFG Ti is lower than that for CG Ti under every HCl solution concentration from 1M to 5M; (ii) for both the UFG and CG Ti samples, the critical current density,  $i_c$  increases with increasing HCl concentration; (iii) the passive current density,  $i_{\text{pass}}$ , of UFG Ti and CG Ti are very similar, and both increases with increasing HCl concentration; (iv) the primary passive potential  $E_P$  shifts to more negative values with increasing HCl

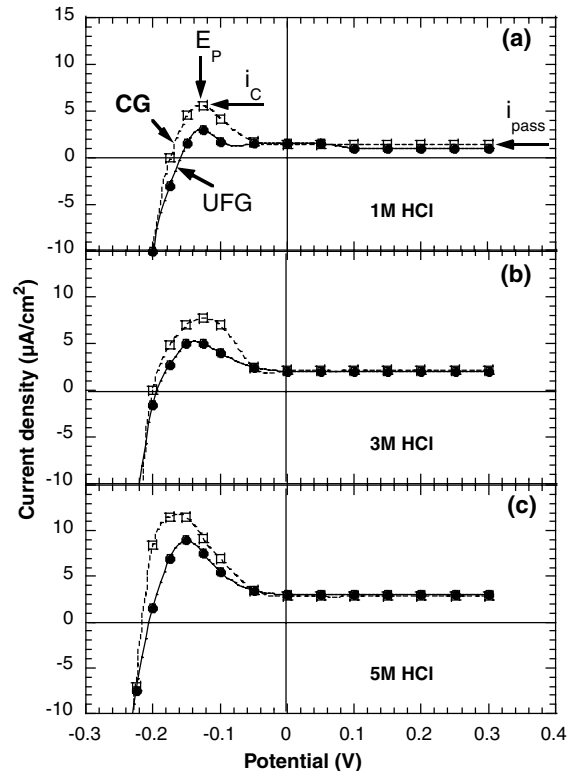


Fig. 1. The polarization curves of UFG and CG Ti in HCl solutions with a concentration of (a) 1M, (b) 3M and (c) 5M. The passive potential,  $E_P$ , critical current density,  $i_c$ , and passive state current,  $i_{\text{pass}}$ , are defined in (a).

Table 1

Corrosion potentials (V), measured under open circuit condition, for CG and UFG Ti measured in HCl and H<sub>2</sub>SO<sub>4</sub> acids

Solution	HCl			H <sub>2</sub> SO <sub>4</sub>		
	1M	3M	5M	1M	3M	5M
CG Ti	+0.193	-0.254	-0.362	+0.237	-0.235	-0.352
UFG Ti	+0.210	-0.242	-0.358	+0.256	-0.223	-0.345
Difference (%)	8.8	4.7	1.1	8.0	5.1	2.0

concentration for CG Ti, but does not shift much for UFG Ti; (v) the full passivation starts at about  $-0.05$  V for both CG and UFG Ti for all solution concentrations.

The polarization curves in  $H_2SO_4$  are shown in Fig. 2. Compared with the polarization curves in Fig. 1, both CG and UFG Ti behave differently in the  $H_2SO_4$  solution, especially at lower  $H_2SO_4$  concentrations of 1M

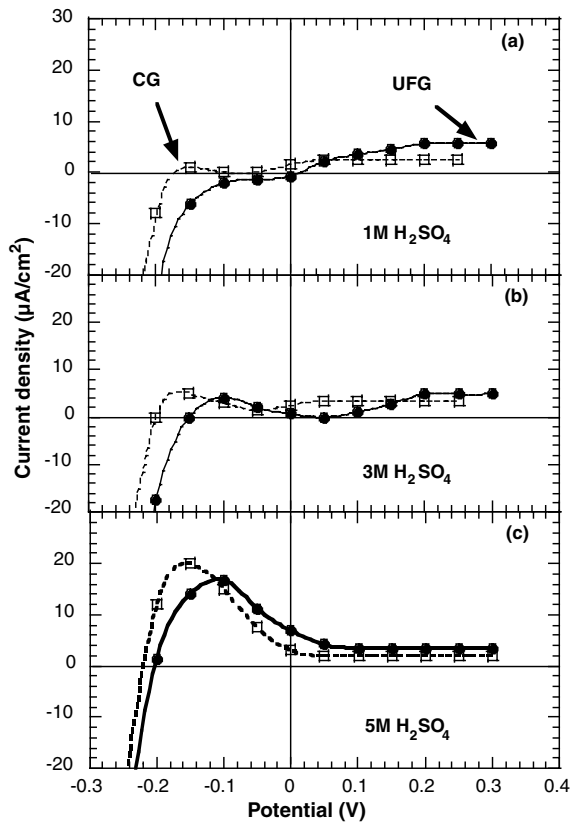


Fig. 2. The polarization curves of UFG and CG Ti in  $H_2SO_4$  solutions with a concentration of (a) 1M, (b) 3M and (c) 5M.

and 3M. The following features can be seen from the polarization curves in Fig. 2: (i) the critical current density,  $i_c$ , for UFG Ti is lower than that for CG Ti for all  $H_2SO_4$  solution concentrations from 1M to 5M; (ii) for both the UFG and CG Ti samples, the critical current density,  $i_c$ , increases with increasing  $H_2SO_4$  concentration; (iii) the passive current density,  $i_{pass}$ , is higher for UFG Ti than for CG Ti, and decreases with increasing  $H_2SO_4$  concentration. The feature (iii) is very different from that in Fig. 1. The passive currents for both UFG and CG Ti in  $H_2SO_4$  solutions are higher than those in HCl solutions.

The corrosion currents were calculated by the four-points method proposed by Jankowski and Juchniweicz [8], and are listed in Table 2. One can see that corrosion current density is lower for UFG Ti than for CG Ti. The difference is in the range of  $3\text{--}7 \times 10^{-6} \text{ cm}^{-2}$ , or 3.1–9.9%.

### 3.3. Corrosion rates

The corrosion rates ( $\text{g/m}^2 \text{ h}$ ) were determined by the weight-loss method. The results are presented in Table 3, which clearly shows that corrosion rates are significantly lower for UFG Ti than for CG Ti in all solutions.

### 3.4. Impurity segregation to grain boundaries in CG Ti

EDS indicated that in CG Ti, impurities including Al and Fe have higher concentrations on grain boundaries than in grain interior. Such segregations were caused by the prolonged annealing of the CG samples at  $800^\circ \text{C}$ . The impurity contents vary from grain to grain and from grain boundary to grain boundary. On average, the Al content is about 40% higher on grain boundary than in grain interior; and the Fe content is 470% higher on grain boundary than in grain interior. Therefore, Fe is much more segregated than Al.

Table 2  
Corrosion current density of UFG Ti and CG Ti ( $\mu\text{m}/\text{cm}^2$ )

	HCl			$H_2SO_4$		
	1M	3M	5M	1M	3M	5M
CG	64	123	169	81	131	157
UFG	61	117	162	73	127	150
Difference (%)	4.7	4.9	4.1	9.9	3.1	4.5

Table 3  
Corrosion rate for UFG Ti and CG Ti,  $\text{g/m}^2 \text{ h}$

Solution	HCl			$H_2SO_4$		
	1M	3M	5M	1M	3M	5M
CG	0.62	1.37	1.98	0.76	1.46	1.87
UFG	0.42	0.90	1.38	0.58	0.78	1.09
Difference (%)	32	34	30	24	47	43

#### 4. Discussions

It is clear from the experimental results that UFG Ti has different corrosion behavior from CG Ti. First, the corrosion potentials of UFG Ti were shifted in the positive direction by 2.0–8.8% in HCl and H<sub>2</sub>SO<sub>4</sub> solutions as compared to the CG Ti (Table 1). The corrosion activation occurs primarily at surface defects such as grain boundaries and dislocations. Although the defect densities in UFG Ti are much larger than in CG Ti, their area fraction on the sample surface is very small as compared with the total surface area. Therefore, only small differences in corrosion potentials were observed.

The corrosion potential does not provide much insight into corrosion rates [9]. The polarization curves give us much more information. It can be seen from Figs. 1 and 2 that the primary passive potential,  $E_p$ , of UFG Ti shifts to more positive value as compared to that of CG Ti, and the critical current densities of UFG Ti are lower than those of CG Ti in both HCl and H<sub>2</sub>SO<sub>4</sub> solutions. These results indicate that UFG Ti might have a lower corrosion rate than CG Ti.

The corrosion current densities (Table 2) determined from the polarization curves using a four-point method [8] indeed demonstrate that the UFG Ti has lower corrosion current densities than CG Ti, although the difference is not large (3.1–9.9%). Table 2 also shows the corrosion current densities increasing with higher acid concentration in both HCl and H<sub>2</sub>SO<sub>4</sub> solutions and for both UFG and CG Ti. However, the relative difference between the corrosion current density of UFG Ti and that of CG Ti was smaller in higher concentration H<sub>2</sub>SO<sub>4</sub> (3M and 5M) than in low concentration H<sub>2</sub>SO<sub>4</sub> (1M), but not affected much by the HCl concentration.

Figs. 1 and 2 show that the passive current density of UFG Ti is similar to that of CG Ti in HCl solutions, but higher than that of CG Ti in H<sub>2</sub>SO<sub>4</sub> solutions. In addition, the polarization curves of UFG and CG Ti samples in the H<sub>2</sub>SO<sub>4</sub> solutions are very complex and different from those in the HCl solutions. These polarization behaviors are not well understood and need further investigation.

The most straightforward measurement of the corrosion resistance of a material is the corrosion rate, which is unfortunately time consuming to measure. Table 3 shows that the corrosion rate of UFG Ti is significantly lower (by 24–43%) than that of CG Ti in all solutions used in this experiment. The corrosion rate increases with increasing acid concentration for both UFG and CG Ti in both HCl and H<sub>2</sub>SO<sub>4</sub> solutions. In the HCl solutions, the relative corrosion rate difference between the UFG and CG Ti samples seems not affected much by the HCl concentration (see Table 3). In contrast, the corrosion rate in CG Ti compared to UFG Ti decreased more significantly in high H<sub>2</sub>SO<sub>4</sub> concentration (3M and 5M) solutions than in the low H<sub>2</sub>SO<sub>4</sub>

concentration (1M) solution. The corrosion rate data in Table 3 clearly establishes that UFG Ti is more corrosion resistant than CG Ti.

The higher corrosion resistance of UFG Ti could be attributed to two factors. First, the segregation of impurities to the grain boundaries in CG Ti could cause intergranular corrosion [9]. Preferential corrosion at grain boundaries could be severe enough to drop grains out of surface, which significantly accelerate the corrosion rate. Second, the UFG Ti, which was deformed severely, could form passive surface layers more readily than CG Ti [10]. Johansen et al. [11] studied Ti oxidation at low current densities and found that Ti oxide film formed on the surfaces of deformed Ti samples (34% plastic strain) at a greater rate than on the surfaces of annealed samples. Tomashov and Ivanov also found lower passivation current,  $i_{pass}$ , for deformed Ti (80% strain) than for annealed Ti [12] in H<sub>2</sub>SO<sub>4</sub> and HCl. It is believed that the passivation first started on surface crystalline lattice defects of Ti [11]. The UFG Ti has high density of grain boundaries and dislocations inside grains. If the passive films on the sample surfaces were nucleated at surface crystalline defects, as asserted in a previous work [11], the UFG Ti would have had a high density of nucleation sites for passive films, which leads to high fraction of passive layers and low corrosion rates.

#### 5. Conclusions

In this study, we found that UFG Ti produced by ECAP had better corrosion resistance than CG Ti in both HCl and H<sub>2</sub>SO<sub>4</sub> solutions. In addition, compared with CG Ti, UFG Ti has lower corrosion current densities, more positive corrosion potential, lower critical currents,  $i_c$ , at the passive potential, and more positive passive potential,  $E_p$ . Higher concentration of HCl or H<sub>2</sub>SO<sub>4</sub> led to higher corrosion rates for both UFG and CG Ti. The corrosion resistance of UFG Ti is believed improved by rapid formation of passive films at surface crystalline defects including grain boundaries and dislocations. On the other hand, the segregation of impurities to grain boundaries in CG Ti could have accelerated its corrosion.

#### Acknowledgements

This research is supported by the IPP program office of the US Department of Energy and the Intas grant no. 01-0320.

#### References

- [1] Valiev RZ, Islamgaliev RK, Alexandrov IV. Prog Mater Sci 2000;45:103.

- [2] Vinogradov A, Mimaki T, Hashimoto S, Valiev RZ. *Scripta Mater* 1999;41:319.
- [3] Rofagha R, Langer R, El-Sherik AM, Erb U, Palumbo G, Aust KT. *Scripta Metall* 1991;25:2867.
- [4] Rofagha R, Erb U, Ostander D, Palumbo G, Aust KT. *Nanostruct Mater* 1993;2:12.
- [5] Thorpe SJ, Ramaswami B, Aust AT. *J Electrochem Soc* 1988;135:2162.
- [6] Schneider M, Zeiger W, Scharnweber D, Woch H. *Mater Sci Forum* 1999;819:225–7.
- [7] Stolyarov VV, Zhu YT, Alexandrov IV, Lowe TC, Valiev RZ. *Mater Sci Eng* 2001;A299:59.
- [8] Jankowski J, Juchniewicz R. *Corros Sci* 1980;20:841.
- [9] Jones DA. *Principals and prevention of corrosion*. 2nd ed. Upper Saddle River, NJ, US: Prentice-Hall, Inc.; 1992.
- [10] Movchan BA, Jakupolska LN. *Prot Met* 1969;5:511.
- [11] Johansen NA, Adams GB, Van Rysseberghe P. *J Electrochem Soc* 1957;104:339.
- [12] Tomashov ND, Ivanov JM. *Prot Met* 1965;1:36.